ELSEVIER

Journal of Power Sources 69 (1997) 125–136

JOURNAL OF POWER SOURCES

The design and construction of high-performance direct methanol fuel cells. 2. Vapour-feed systems

Martin Hogarth [1], Paul Christensen *, Andrew Hamnett, Ashok Shukla [2]

Department of Chemistry, Bedson Building, The University of Newcastle, Newcastle upon Tyne NE1 7RU, UK

Received 15 July 1996; revised 13 February 1997

Abstract

The construction of a gas-fuel-feed direct methanol fuel cell is described in detail and the optimisation of the active electrode fabrication process is also reviewed. For this vapour phase-system, it has proved possible to develop a Nafion™ encapsulated process in which the porous carbon electrodes were bonded with Nafion™ rather than polytetrafluoroethylene (PTFE). Initially, PTFE was removed only from the anode paste, but it was found that PTFE was also unnecessary at the cathode. The best performance was found for extremely thin catalysed carbon layers at the two electrodes, and to reduce loadings, thin layers of uncatalysed carbon were inserted between the carbon cloth current collectors and the catalysed carbon layers. The final electrodes had loadings of 2 mg cm^{-2} on the anode and 0.5 mg cm^{-2} on the cathode and gave peak power densities of 0.35 W cm^{-2} with oxygen and 0.22 W cm^{-2} with air as the combustant. © 1997 Elsevier Science S.A.

Keywords: Fuel cells; Direct methanol fuel cells; Vapour-feed systems

1. Introduction

In the previous paper [1], the performance of a variety of membrane-electrode assemblies (MEAs) in a prototype liquid-feed direct methanol fuel cell (DMFC) was described. The DMFC has attracted considerable attention in the last few years [2] since it offers, at least potentially, an alternative and relatively simple power source for transport. Attention has particularly focused on DMFC cell designs with solid polymer electrolytes (SPE) such as Nafion™, since such cells offer considerable engineering advantages. However, there remain real problems with the realisation of this type of fuel cell, even in the SPE configuration, as discussed in the previous paper. However, improvements in the anode performance in the last few years have led to the view that even with these recognised drawbacks, efforts should be made to construct complete cell prototypes for testing [3–6].

As indicated previously, the key to cell construction is the MEA that lies at the heart of the fuel cell system. Optimisation of this MEA can only be carried out within the confines of the overall system, including not only the design of the mechanical framework but also the central decision as to whether the fuel is supplied as a liquid or a vapour. In the previous paper, we considered the first of these cases, that of liquid-feed, and compared the advantages and disadvantages of liquid- and vapour-feed systems. In this paper, we turn to the provision of the fuel as the vapour, and explore the problems associated with this type of system.

In addition to the fuel supply system, vapour-phase cells are also very sensitive to the pressure on the cathode side, and considerable effort has gone into the design and construction of more sophisticated controlled pressure systems than those necessitated by our initial studies on liquid-feed cells. Although the same caveats apply to pressurised vapour-feed systems as liquid-feed systems, the effect of pressure on performance, particularly for methanol/air cells, is so great that parasitic losses associated with the compressor system are more than likely to be paid back by enhanced overall efficiencies.

As for the liquid-feed system already described, the vapour-feed cell system has been constructed with certain fundamental material requirements in mind. These are very similar to the constraints described in the previous paper,

* Corresponding author: Tel.: +44 (91) 222 67 86; Fax: +44 (91) 222 69 29.

[1] Present address: Johnson Matthey Technology Centre, Blount's Court, Sonning Common, Reading RG4 9NH, UK.

[2] On leave from the Solid State and Structural Chemistry Unit, Indian Institute of Science, Bangalore-560012, India.

PII S0378-7753(97)02581-0

with low-corrosion materials of good thermal conductivity essential.

Using a vaporised fuel has, in principle, a number of advantages over liquid fuel in terms of performance. In the gas phase, both mass transport and electrode kinetics are enhanced, resulting in significant increases in cell performance. It was anticipated that using hot methanol/water vapour mixes at 200 °C would produce localised heating of the electrode assembly, but this was not observed. Our vapour-feed cell is described in detail below, and early performance indicators from the cell suggest that with suitable choice of design parameters, extremely encouraging data can be obtained.

2. Experimental

2.1. Cell construction

The most primitive form of gas-fuel-feed system involves the use of an inert carrier gas, such as nitrogen, to facilitate the circulation of both methanol and water vapours around the cell. A sealed glass reservoir of the methanol/water mixture was externally heated and maintained at 60 °C using heating pads (Watlow 240 V 150 W). Nitrogen was supplied from a pressurised cylinder using a regulator and a needle valve to control the flow rate. The nitrogen was introduced into a tightly wound glass coil which was submerged to a depth of 20 cm in the fuel mixture. A porous glass sinter was located in the opposite end of the coil to act as an atomiser. The resulting gas mixture was directed into the anode compartment of the fuel cell and waste products were collected in a separate reservoir.

This method had the advantage of simplicity, but the rate of supply of methanol was difficult to control, and the nitrogen gas acted as a diluent, with the result that attention turned quickly to the flash-vaporisation of the methanol/water mixture on a hot surface, with the resulting super-heated gases being directed into the anode compartment of the cell. A block diagram of the flash vapour system is shown in Fig. 1.

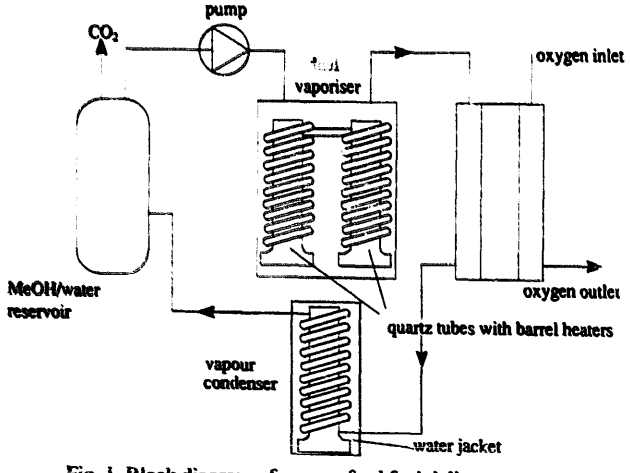

Fig. 1. Block diagram of vapour-feed fuel delivery system.

The methanol/water mixture was pumped into a pair of heated quartz coils using a peristaltic pump and the resulting vapour directed into the cell. The double-quartz coil configuration ensured complete vaporisation of the fuel, producing a more homogeneous jet. The quartz coils were heated using 100 W barrel heaters, and a thermocouple junction was attached to the vapour outlet tube to determine the temperature of the emerging vapour. By means of feedback electronics, the methanol/water vapour temperature was kept constant at 200 °C. The vapour flow rate was determined with the pump flow rate setting. A fuel recovery system was employed, in which the exhaust vapour from the cell was passed into a water-cooled condensing coil, and the resulting liquid pumped into the fuel reservoir. In this way the cell could be operated for many hours on a single reservoir of fuel.

As for the liquid-feed system, control of the pressure in a vapour-feed DMFC is of considerable potential importance. The early manometer system developed for liquid-feed systems proved unreliable at practical pressures, and a second pressurisation system was constructed from high pressure stainless-steel gas fittings instead of the silicone rubber tube fittings previously employed, as shown in Fig. 2. The fittings were screwed directly into the field plates of the cell, together with a neoprene rubber gasket to obtain an excellent gas seal. A second, dedicated fine adjustment needle valve was used to control the cell pressure and the water produced at the cathode could escape past the valve into a reservoir. Pressures in excess of 5 bar were easily attained with this improved configuration and the cell pressure could be conveniently monitored with the integrated pressure gauge.

The design specification of the cell used for the vapour-feed experiments is shown in Fig. 3, and is a development of the liquid-feed cell described in the previous paper. The field plates were constructed in graphite rather than the PTFE–mica composite used in the liquid-feed cell, and offered a more rigid support for the electrode. Instead of using a graphite paper flow channel, a flow channel was cut directly into

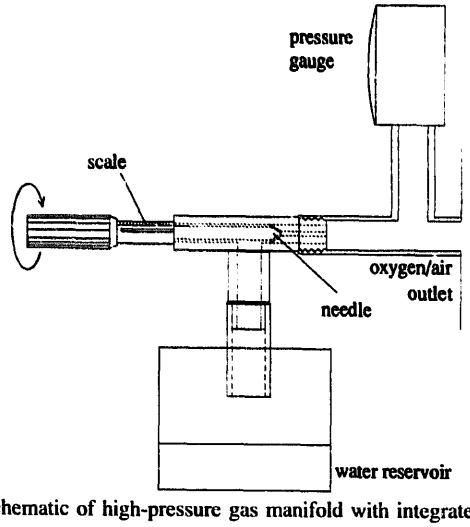

Fig. 2. Schematic of high-pressure gas manifold with integrated pressure gauge.

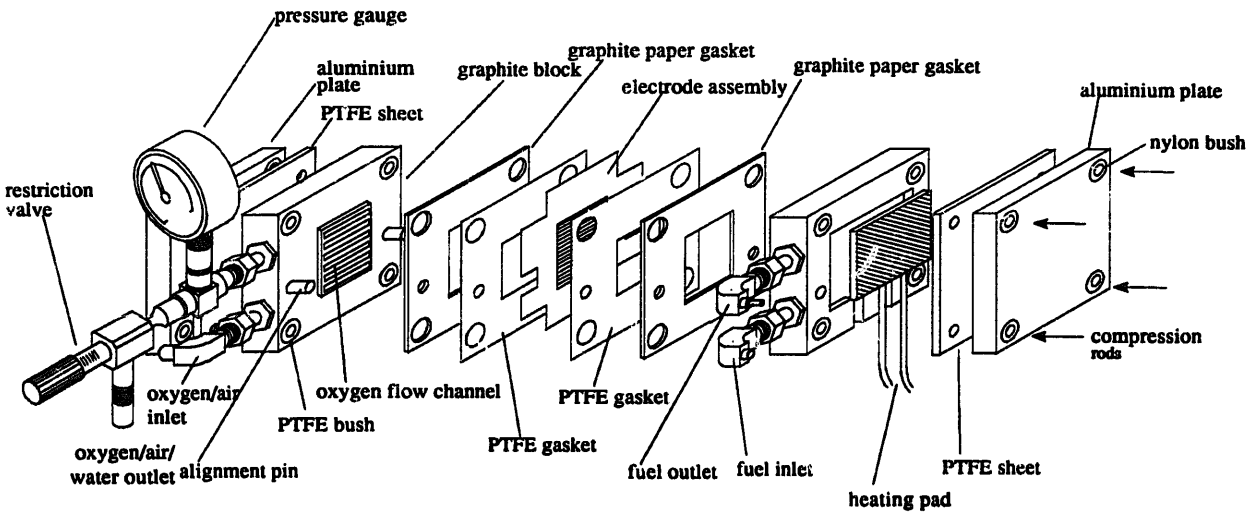

Fig. 3. Design specification of vapour-feed cell.

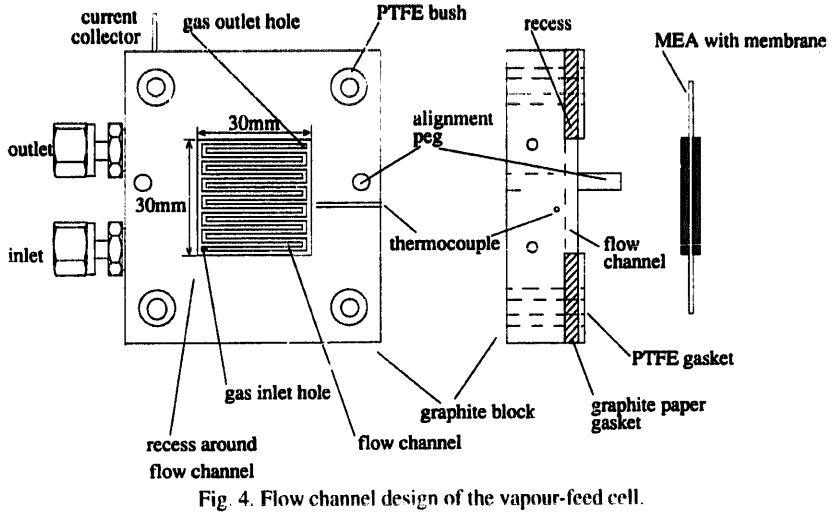

Fig. 4. Flow channel design of the vapour-feed cell.

each graphite block to a depth of 1 mm to the design shown in Fig. 4. Two alignment pins were again employed to aid in the alignment of the various gaskets and the electrode assembly. It was necessary to provide additional insulation in the form of PTFE bushes at each corner of the graphite block to prevent electrical shorting when the compression rods were inserted. A gas seal was made using two graphite paper sheets (Papyex-N paper, Le Carbone) which were cut with a 9 cm^2 hole so as not to cover the flow channels on the graphite plates, and two PTFE gaskets, which presented 6 cm^2 of electrode area. However, the current densities were adjusted to 2 cm^2 which corresponds to the open channel area of the flow pattern. The graphite plates were recessed around the flow channel to the depth of the graphite paper so that the graphite paper gasket, when in position, was level with the ribs of the flow channel. Each graphite plate had two bore holes in one of its narrow sides into which the fuel and oxidant systems were fitted. The bore holes emerged at right angles, out through the front face of the block at opposite corners of the flow channel pattern.

Cell heating was accomplished using two integrated heating pads, and offered temperature control across the 25–120 °C range. A screw embedded into each graphite block acted as the current collectors for connection to the external load.

The majority of sealing problems experienced with the liquid-feed cell were solved in this second design. In particular, cell pressurisation was effected up to pressures of 5 bar without leakage. Both fuel and oxidant were supplied from the bottom portion of the cell, up through the flow channel and out of the upper portion of the cell. This configuration prevented drying of the cathode, and any excess water was transported through the manifold into a reservoir.

2.2. *Electrode fabrication*

Electrodes and membrane electrode assemblies were fabricated with methods similar to those described in the previous paper, with one important difference. For the vapour-feed system, it proved possible to develop a Nafion® encapsulated process in which the porous carbon electrodes were bonded with Nafion®, and contained no PTFE. This allowed electrodes to be fabricated with very thin, highly loaded, catalysed carbon layers, in order to reduce ohmic losses and increase catalyst utilisation.

2.3. Electrodes of type D

The anode layer was prepared with only a Nafion® binder. A weighed quantity of catalysed carbon was carefully mixed with 100 mg of Nafion® solution (5 wt.%, Aldrich) and a small quantity of isopropanol and water (1:2) to give a thin ink-like paste. The ink was allowed 30 min to soak in the Nafion® solution before being carefully spread onto a carbon cloth to a thickness of about 0.5 mm and geometric area 9 cm^2.

The cathode layer was prepared by mixing a weighed quantity of catalysed carbon with a PTFE suspension and a small quantity of isopropanol and water (1:2). The carbon/PTFE ink was carefully mixed manually for 15 min to give a putty-like material, and then spread onto a carbon cloth to a thickness of about 1 mm and geometric area 9 cm^2. Following this, the cathode was cold pressed for 10 min under a load of 100 kg cm^{-2} followed by sintering at 350 °C for 30 min.

Both electrodes were given 2 brush coats of Nafion® solution to give the required loadings and were allowed to dry in air for 10 min before being assembled with a Nafion® membrane. The complete electrode assembly was placed between two stainless-steel plates with a non-stick paper backing and gradually heated over a 5-min period to 135 °C under a load of 1 kg, and compacted at 75 kg cm^{-2} for 3 min. Following compaction, the electrode assembly was immediately soaked in cold Millipore conductivity water for 2 h prior to mounting in the cell.

Table 1 summarises the composition and the compaction conditions used during electrode manufacture [11]. The anode layer consisted of a 60 wt.% Pt–Ru catalyst and the cathode a 40 wt.% Pt catalyst with the Pt loadings maintained at 5 mg cm^{-2} on each electrode.

2.4. Electrodes of type E

The encouraging results for electrodes of type D led naturally to MEAs in which PTFE was removed from both the anode and the cathode. The anode and cathode electrodes were prepared identically as follows.

A weighed quantity of catalysed carbon was carefully mixed with 100 mg of Nafion® solution and a small quantity of isopropanol and water (1:2) to give a thin ink. The ink was allowed 30 min to soak in the Nafion® solution before being carefully spread onto a carbon cloth to a thickness of about 0.5 mm and geometric area 9 cm^2. The electrode was then brush coated with 2 coats of Nafion® solution to give the required loading, and allowed to dry for 10 min before being assembled with a Nafion® membrane. The complete electrode assembly was placed between two stainless-steel plates with a non-stick paper backing and gradually heated over a 5-min period to 135 °C under a load of 1 kg, and compacted at 75 kg cm^{-2} for 3 min. Following compaction the electrode assembly was immediately soaked in cold Millipore conductivity water for 2 h prior to mounting into the cell.

Table 2 summarises the compositions and compaction conditions used during electrode fabrication. Both E-type electrodes contained a Pt loading of 5 mg cm^{-2} on the anode, and 3 mg cm^{-2} (E2) or 5 mg cm^{-2} (E1) on the cathode. Electrode E1 was prepared from a 60 wt.% Pt–Ru catalyst for the anode and a 40 wt.% Pt catalyst for the cathode. Electrode E2 was, however, prepared from an 80 wt.% Pt–

Table 1
Summary of compaction conditions and electrode compositions of MEA D1

	Electrode composition		Pressing conditions
	Anode	Cathode	
D1 [a]	60wt.%Pt–Ru (5 mg Pt cm^{-2}) 1.1 mg Nafion® cm^{-2}	40 wt.% Pt (5 mg Pt cm^{-2}) 15 wt.% PTFE 0.8 mg Nafion® cm^{-2}	75 kg cm^{-2} 135 °C 180 s

[a] Cathode compacted under 100 kg cm^{-2} for 10 min prior to sintering.

Table 2
Summary of compaction conditions and electrode compositions of MEAs E1 and E2

	Electrode composition		Pressing conditions
	Anode	Cathode	
E1	60wt.%Pt–Ru (5 mg Pt cm^{-2}) 1.7 mg Nafion cm^{-2}	40 wt.% Pt (5 mgPt cm^{-2}) 1.4 mg Nafion cm^{-2}	75 kg cm^{-2} 135 °C 180 s
E2	80wt.%Pt–Ru (5 mg Pt cm^{-2}) 1.4 mg Nafion cm^{-2}	60 wt.% Pt (3 mg Pt cm^{-2}) 1.1 mg Nafion cm^{-2}	75 kg cm^{-2} 135 °C 180 s

Ru catalyst for the anode and 60 wt.% Pt catalyst for the cathode.

2.5. Electrodes of type F

The performance of electrodes of type E shows a further marked improvement, arising from the implementation of extremely thin, highly loaded catalyst layers bonded directly to the Nafion® membrane. However, there is a lower limit to the thickness with which a carbon layer can be spread onto a carbon cloth because of the cloth's absorbing nature. This was a particular problem at the anode when using the 80 wt.% Pt–Ru catalyst, which contains very little carbon. The problem is further complicated if the catalyst loading is to be lowered, since the quantity of catalysed carbon is reduced and is hence more difficult to spread onto the carbon cloth. These problems have been reduced to a large extent by modifying the electrode structure through the insertion of an uncatalysed porous carbon layer between the catalyst layers and the carbon cloth, giving a less absorbent base to spread the catalyst inks and a suitable gas diffusion layer. Consequently, the catalyst loadings were reduced, yielding electrodes which contained a catalyst layer of only about 100 μm thickness.

The laminar configurations of the composite electrode and standard electrode used within MEAs are shown in Fig. 5. A catalyst layer prepared from 15 wt.% Pt catalyst (0.5 mg cm^{-2}) was bonded directly onto the membrane, and an uncatalysed carbon gas diffusion layer was then placed on this catalyst layer. The electrode was prepared as follows.

Two carbon inks were prepared as previously described for electrodes of type E. The uncatalysed carbon ink was prepared by mixing 50 mg of uncatalysed carbon black (Ketjen EC600-JD) with 50 mg of Nafion® solution and a small quantity of Millipore conductivity water and isopropanol (2:1). Simultaneously, a catalysed carbon ink was prepared by mixing the required quantity of catalysed carbon with 50 mg of Nafion® solution and a small quantity of Millipore conductivity water and isopropanol (2:1). After 30 min (to allow Nafion® to be absorbed by the carbon), a thin layer (~0.25 mm) of the uncatalysed carbon ink was spread onto a carbon cloth of area 9 cm^2. The catalysed carbon ink was immediately spread on top of this uncatalysed layer and the electrode was then brush-coated with two coats of Nafion® solution, and compacted as previously described above.

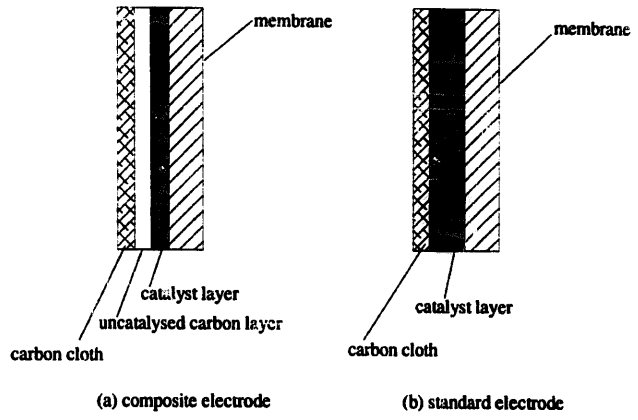

Fig. 5. Comparison of standard and composite electrode configurations.

Two MEAs have been fabricated with this technique: the first has the anode prepared as a single layer and the cathode as a composite layer. The second has both electrodes prepared as composites.

Table 3 summarises the composition and the compaction conditions used during electrode manufacture. For MEA F1, the anode was prepared as for electrodes of type E, from 70 wt.% Pt–Ru, with the Pt loading maintained at 5 mg cm^{-2}, but the cathode was prepared as a two-layer composite with a Pt loading of 0.5 mg cm^{-2}. For electrode F2, the composite anode was prepared from 70 wt.% Pt–Ru catalyst with a Pt loading of 2 mg cm^{-2}, and the composite cathode was prepared from 15 wt.% Pt catalyst with a Pt loading of 0.5 mg cm^{-2}.

3. Results and discussion

3.1. Electrodes of type D

Fig. 6(a) and (b) shows the performance of electrode D1 operating in the vapour-feed cell at 97 °C with 2 M methanol and oxygen at a pressure of 1.5 bar. The data, which are not *iR*-corrected, show a very high electrode performance for D1,

Table 3
Summary of compaction conditions and electrode compositions of MEAs F1 and F2

	Electrode composition		Pressing conditions
	Anode	Cathode	
F1 [a]	70wt.%Pt–Ru (5 mg Pt cm^{-2}) 1.4 mg Nafion® cm^{-2}	15 wt.% Pt (0.5 mg Pt cm^{-2}) 1.1 mg Nafion® cm^{-2}	75 kg cm^{-2} 135 °C 180 s
F2 [a]	70wt.%Pt–Ru (2 mg Pt cm^{-2}) 1.1 mg Nafion® cm^{-2}	15 wt.% Pt (0.5 mg Pt cm^{-2}) 1.1 mg Nafion® cm^{-2}	75 kg cm^{-2} 140 °C 180 s

[a] Nafion® loading including uncatalysed carbon layer for composite electrode.

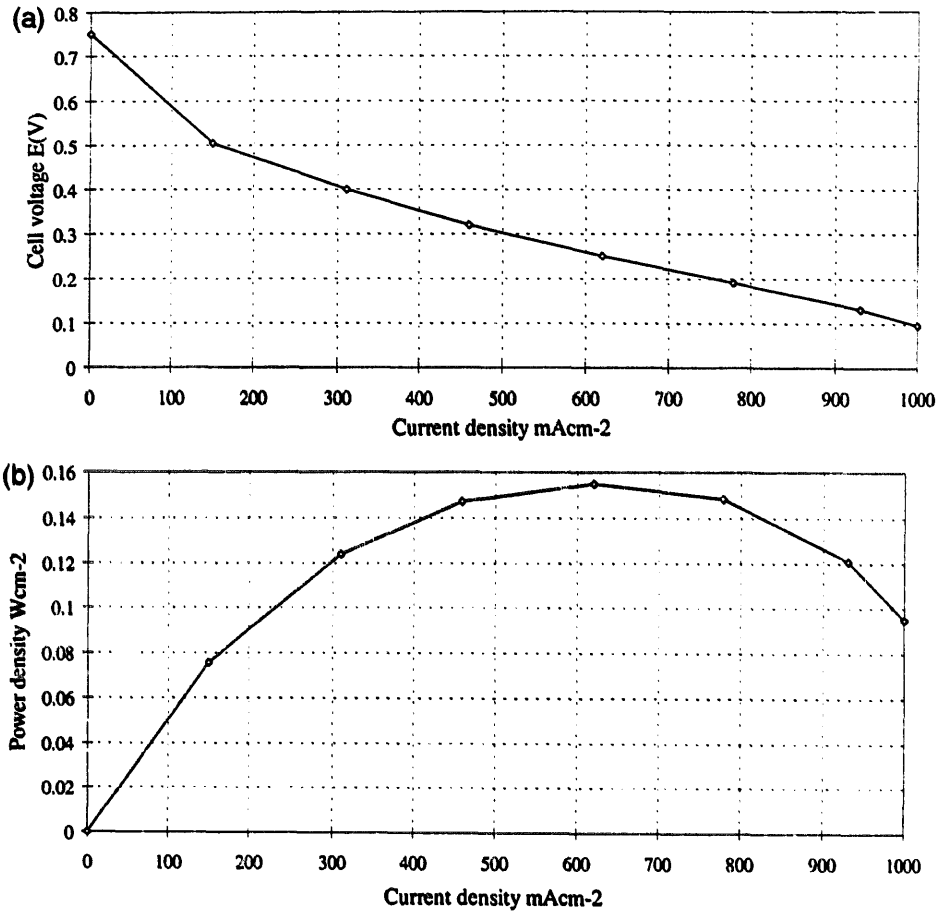

Fig. 6. (a) Polarisation curve for electrode D1 operating in the vapour-feed cell at 97 °C with 2 M aqueous methanol at the anode and oxygen at 1.5 bar pressure at the cathode. (b) Power density data for the cell of Fig. 6(a).

with cell voltages of 0.58 and 0.47 V at 100 and 200 mA cm^{-2}, respectively. The performance of the electrode assembly was particularly impressive at higher current densities, with cell voltages of 0.3 and 0.1 V at current densities of 500 and 1000 mA cm^{-2}, respectively. The electrode produced a maximum power density of 0.155 W cm^{-2} which is nearly double the value attained for the previous electrode type operating with liquid methanol. This level of performance was very encouraging, even though relatively high catalyst loadings were required on the both the anode and cathode to attain this level.

Fig. 7 shows the results of life-time tests carried out with electrode D1 over a 8-h period. Evidently there is very little degradation of the cell voltage over this time period at the load currents used. This suggests that long-term poisoning of the cathode from methanol permeation was not as serious a problem as expected [2].

The performance of electrode D1 was very high in comparison to the previous electrode types explored in the liquid-feed cells. A peak power output of 0.155 W cm^{-2} was recorded at a current loading of ~600 mA cm^{-2}, which is double the performance of electrode C1 in the previous paper. Importantly, endurance testing of the electrode showed no serious deterioration in cell performance. The initial problems of high ohmic losses and low ionic conductivities appear to have been overcome to a large extent. This has come about through much improved contact between the porous carbon layers and the Nafion® membrane, and a reduction in the thickness of the porous carbon layers.

3.2. *Electrodes of type E*

Fig. 8(a) and (b) shows the gradual change in performance of the Nafion® encapsulated electrode assembly (E1) over a period of 77 h, operating at 97 °C with a methanol feed and oxygen at a pressure of 1.5 bar. The initial activity of the electrode was quite poor, but after 77 h the electrode performance reached a peak performance of 0.3 and 0.1 V at current densities of 500 and 1000 mA cm^{-2}, respectively. Open-circuit potentials in excess of 0.9 V were recorded which are comparatively high to those reported in our previous and earlier papers [7–9], and the peak power density was seen to increase from its initial value of ~0.03 W cm^{-2} to the more respectable value of 0.15 W cm^{-2} after 77 h continuous operation, a fivefold increase in magnitude.

There is a number of possible rationales that could account for the extended periods required for electrode conditioning. The most likely is that the electrode becomes severely dehydrated during electrode compaction. It is also possible that there are some residual alcohols from the Nafion® solution

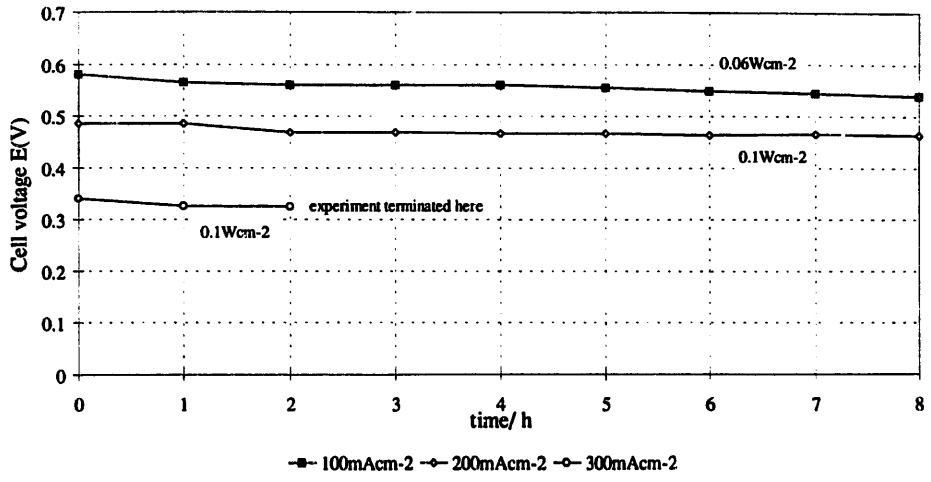

Fig. 7. Lifetime tests for the cell of Fig. 6(a) over an 8-h period and different current densities.

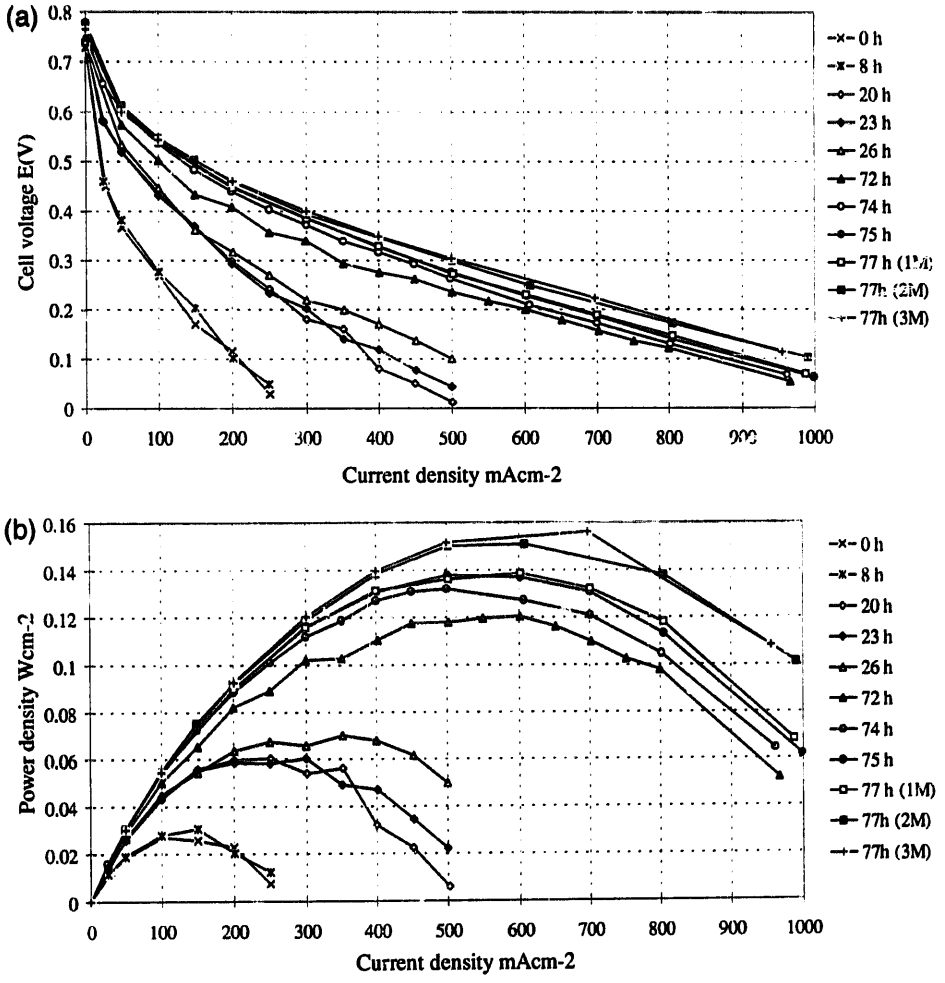

Fig. 8. (a) Polarisation data for the Nafion® encapsulated electrode assembly E1 over a period of 77 h operating at 97 °C with 2 M aqueous methanol, and oxygen at 1.5 bar. (b) Power density for the cell of Fig. 8(a).

which remain locked within the pores of the electrode. The porous structure of the electrode may also change during the conditioning process, with more catalyst becoming accessible to methanol and oxygen following extended periods of operation.

One obvious and important consideration is the high catalyst loadings used in electrode E1. The anode contained 5 mg Pt cm^{-2} and 2.5 mg Ru cm^{-2}, while the cathode contained 5 mg Pt cm^{-2}. Consequently, electrode E2 was fabricated with a reduced platinum loading of 3 mg Pt cm^{-2} on the cathode. The catalyst layers were also reduced in thickness by using more highly loaded catalysed carbons, in an attempt to reduce ohmic losses. An 80 wt.% Pt–Ru catalyst was used for the anode and a 60 wt.% Pt catalyst for the

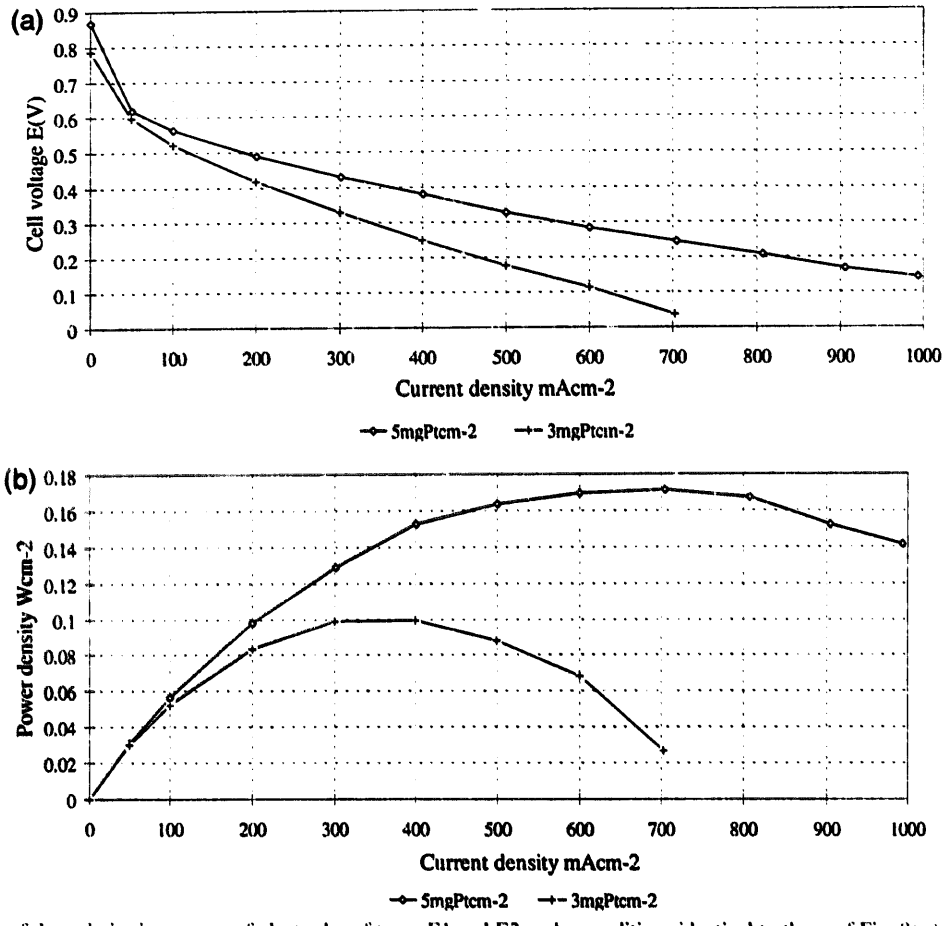

Fig. 9. (a) Comparison of the polarisation curves of electrodes of types E1 and E2 under conditions identical to those of Fig. 8(a). (b) Comparison of the power density data for electrodes of types E1 and E2.

cathode with correspondingly reduced Nafion® loadings to account for the change in electrode thickness (see Table 2). Fig. 9(a) and (b) compares the performance of electrodes E1 and E2 operating in the vapour-feed cell at 97 °C with 2 M methanol and 1.5 bar oxygen pressure. Electrode E1 gave cell voltages of 0.33 and 0.14 V at 500 and 1000 mA cm^{-2}, respectively, with a peak power density of 0.17 at 700 mA cm^{-2}. The performance of electrode E2 was significantly poorer, giving a cell voltage of just 0.18 V at 500 mA cm^{-2} with a corresponding peak power density of 0.1 W cm^{-2} at 350 mA cm^{-2}.

The area resistances in electrode assemblies of type E were reduced considerably, to values around 0.3 Ω cm^2 by removing the PTFE binder, and the carbon structure of the electrodes appeared to be more compact without the PTFE binder, possibly leading to more intimate contact between the macroscopic carbon black particles. Unfortunately, the data also illustrate the dramatic decrease in electrode activity when the Pt loading on the cathode was reduced to 3 mg cm^{-2}. When the cathode oxygen pressure was increased above 3 bar, the electrode performance was not enhanced as expected, but began to fall. This suggests that the cathode was flooding which reduced the accessibly of the oxygen to the catalyst. This is not surprising given that the cathode contained no PTFE to control its hydrophobicity.

3.3. Electrode of type F

The flooding problems and fabrication difficulties for electrodes of type E have led us to composite structures of type F as described above. Fig. 10(a) and (b) shows the performance of electrode F1 after 120-h operation in vapour-feed cell at 97 °C with 2 M aqueous methanol feed and oxygen at a pressure of 3 bar.

The performance of electrode F1 was very exciting; it showed the successful implementation of a composite cathode containing only 0.5 mg Pt cm^{-2}. The measured cell voltages were 0.3 and 0.1 V at 500 and 1000 mA cm^{-2}, respectively, with a peak power density of 0.155 W cm^{-2} at 600 mA cm^{-2}. This level of performance was very similar to that of electrode E1 which contained a standard cathode with a Pt loading of 5 mg cm^{-2}, and substantially better than that of electrode E2 which contained a standard cathode with a Pt loading of 3 mg cm^{-2}.

The area resistance of the electrode was quite small at 0.48 Ω cm^2, though this is a small increase from electrode E1. Fig. 11 shows the results of life-time testing of electrode

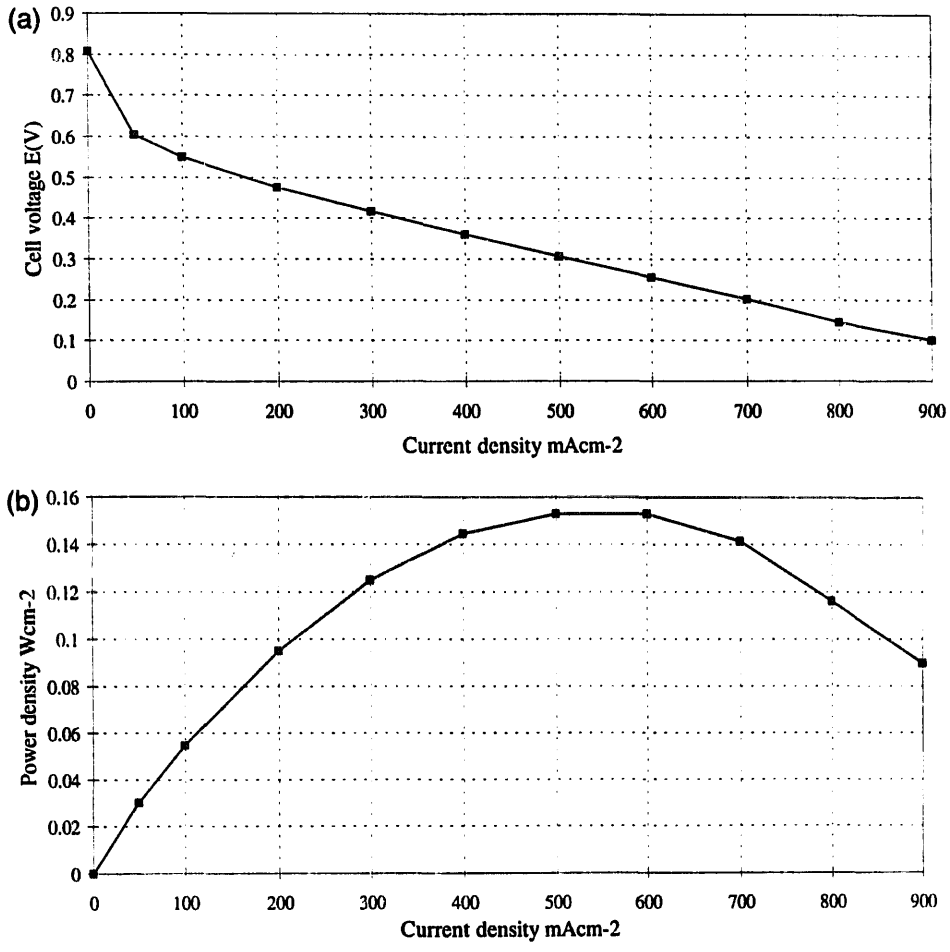

Fig. 10. (a) Polarisation data for composite electrodes of type F1 at 97 °C with 2 M aqueous methanol and oxygen at a pressure of 3 bar. (b) Power density data for the electrode of Fig. 10(a).

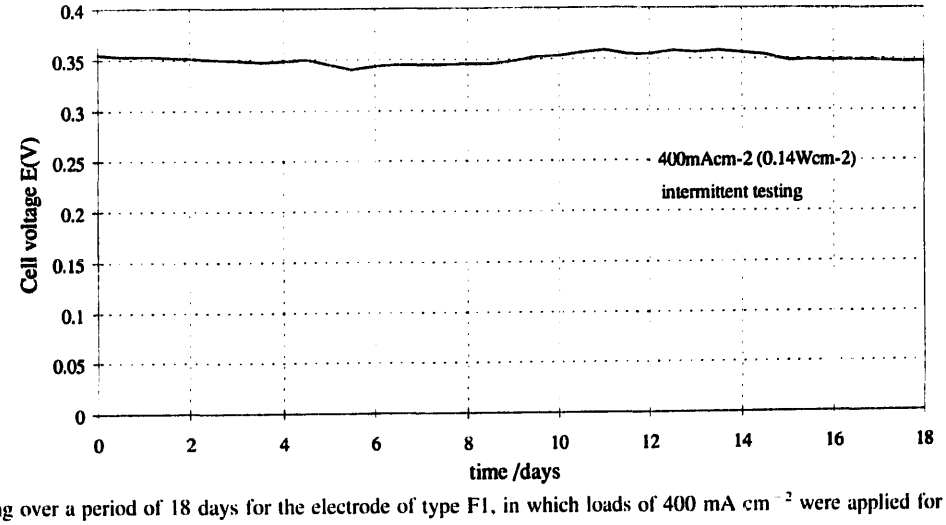

Fig. 11. Lifetime testing over a period of 18 days for the electrode of type F1, in which loads of 400 mA cm^{-2} were applied for periods of several hours on-and-off to simulate driving loads.

F1 over an 18-day period at an intermittent load of 400 mA cm^{-2} (0.14 W cm^{-2}). The data do not show any significant degradation of the cell voltage.

Clearly, the fabrication of a composite cathode has aided in the dramatic reduction of catalyst loadings. The electrode performance was little affected when the Pt loading was reduced from 5 to 0.5 mg cm^{-2}, and the success of this composite electrode strategy for the cathode side led us to prepare both electrodes in the MEA as composites.

Figs. 12(a), (b) and 13 show the performance of electrode F2 in the vapour-feed cell at 97 °C with 2 M methanol at a variety of oxygen pressures. The cell voltage was seen gradually, but not dramatically, to increase at higher oxygen gas pressures. For example, the cell voltages were 0.37 and

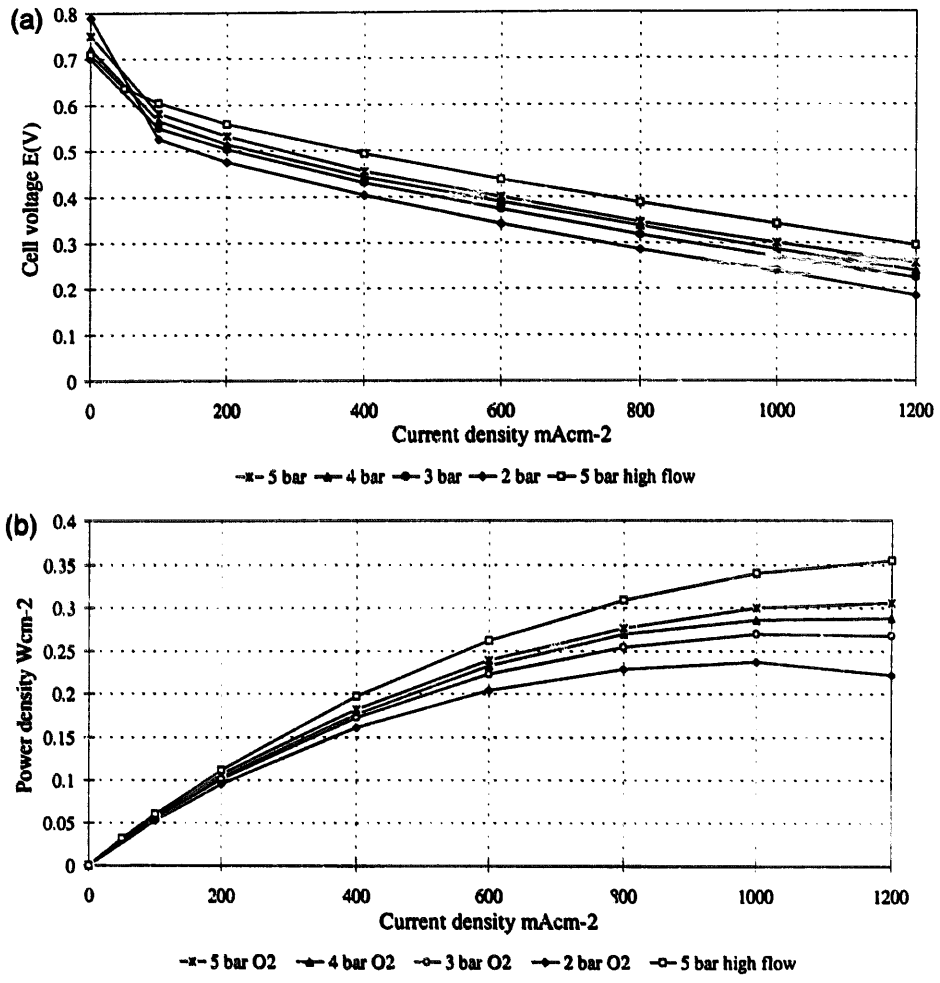

Fig. 12. (a) Polarisation data for electrode F2 in the vapour-feed cell at 97 °C with 2 M methanol at different oxygen pressures. (b) Power density data for the cell of Fig. 12(a).

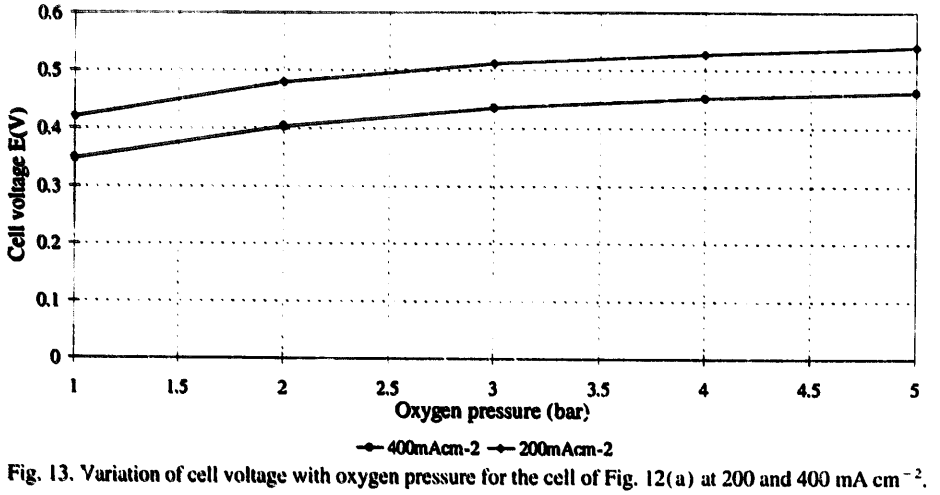

Fig. 13. Variation of cell voltage with oxygen pressure for the cell of Fig. 12(a) at 200 and 400 mA cm^{-2}.

0.24 V at current loadings 500 and 1000 mA cm^{-2}, with a peak power density of 0.24 W cm^{-2}, when the cathode was pressurised at 2 bar. The cell voltages increased to 0.43 and 0.3 V and the peak power density to 0.31 W cm^{-2} as the oxygen pressure was increased to 5 bar. The highest performance was attained at 5 bar oxygen pressure with a high oxygen flow rate. The cell voltages increased to 0.46 and 0.34 V with a maximum power density of > 0.35 W cm^{-2}. This behaviour suggests that the cathode might be flooding, and that the high gas flow aided the removal of the water from the electrode pores. It is also possible that the higher oxygen pressure inhibited the permeation of methanol from the anode.

The cell voltage was seen to increase, for both load currents, as the oxygen pressure was increased. However, the cell performance when operating with pressurised air is of greater practical interest, and Fig. 14(a) and (b) presents

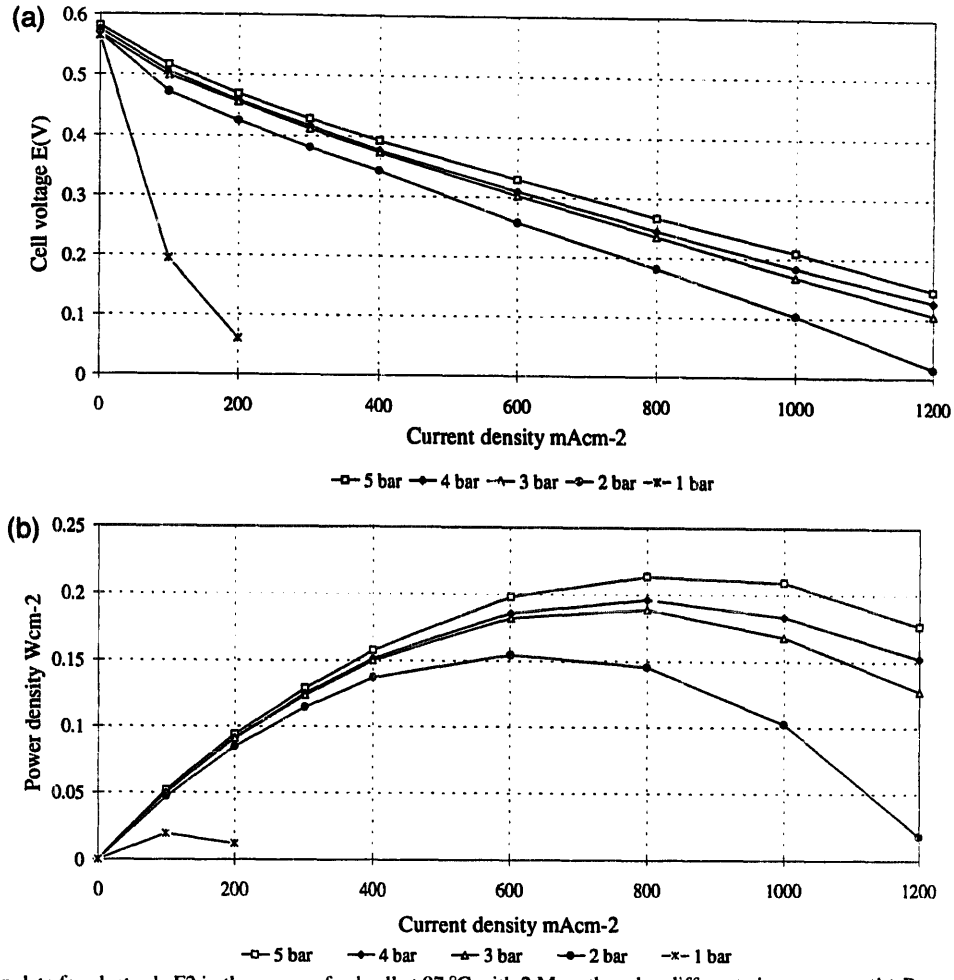

Fig. 14. (a) Polarisation data for electrode F2 in the vapour-feed cell at 97 °C with 2 M methanol at different air pressures. (b) Power density data for the cell of Fig. 14(a).

data for the same electrode assembly operating with air at a variety of pressures. The open-circuit potential was seen to fall from about 0.8 to 0.6 V with air. The extent of cathode pressurisation can also be seen to have a more dramatic effect on the cell performance than observed with oxygen. At 1 bar pressure, severe concentration/mass transport limitations were responsible for a dramatic decline in the cell performance for the methanol/air cell. The highest activity was attained again at 5 bar air pressure, the cell voltages were 0.37 and 0.2 V at current loadings of 500 and 1000 mA cm^{-2}, the peak power density was 0.22 W cm^{-2} at a current loading of 800 mA cm^{-2}. The area resistance of the electrode assembly when operating with oxygen was 0.21 Ω cm^2, which is a similar to the values attained by H_2/O_2 cells [9–11].

4. Conclusions

Evidently, the performance of our gas-feed systems exceeds by some margin the performance of the liquid-feed systems described in the previous paper. Furthermore, application of composite anodes and cathodes have led to considerable reductions in the catalyst loadings. Electrode F2 contained Pt loadings of 2 mg cm^{-2} on the anode and 0.5 mg cm^{-2} on the cathode. This electrode configuration attained a very high performance, producing peak power densities in excess of 0.35 W cm^{-2} with oxygen and 0.22 W cm^{-2} with air. More importantly, the electrode was capable of generating high power densities at useful cell voltages. With oxygen and at a cell voltage of 0.5 V, the current density was 400 mA cm^{-2} which corresponds to a power density of 0.2 W cm^{-2}. Similarly with air and at a cell voltage of 0.4 V, the current density was 400 mA cm^{-2} which corresponds to a power density of 0.16 W cm^{-2}.

Acknowledgements

We gratefully acknowledge the Royal Society for a Visiting Fellowship to A.S., and the EPSRC for a studentship (to M.P.H.) and a post-doctoral fellowship (to A.S.). We are also grateful to the EU for funding under the Joule II project.

References

[1] M.P. Hogarth, P.A. Christensen, A. Hamnett and A.K. Shukla, *J. Power Sources*, to be published.

[2] A. Hamnett and G.L. Troughton, *Chem. Ind.*, (6 July) (1992) 480.

[3] M.P. Hogarth, J. Munk, A.K. Shukla and A. Hamnett, *J. Appl. Electrochem.*, *24* (1994) 85.

[4] P.K. Shen and A.C.C. Tseung, *Ext. Abstr., Proc. 186th Meet. The Electrochemical Society, Spring. Meet., Hawaii, HI, USA, 16–21 May 1993*, Proc. Vol. 93-1, Abstr. No. 576.

[5] M.P. Hogarth, P.A. Christensen and A. Hamnett, *Proc. 1st Int. Symp. New Materials for Fuel Cell Systems, Montreal, Canada, July 1995*, pp. 310–325.

[6] A.S. Aricò, V. Antonucci, N. Giordano, A.K. Shukla, M.K. Ravikumar, A. Roy, S.R. Barman and D.D. Sharma, *J. Power Sources, 50* (1994) 295.

[7] EU Contractors Meeting, *Project JOUE-CT92-0102*, Siemens GmbH, Germany, June 1994.

[8] S. Surampudi, S.R. Narayanan, E. Varmos, H. Frank, G. Halpert, A. LaConti, K. Kosek, G.K. Surya Prakesh and G.A. Olah, *J. Power Sources, 47* (1994) 337–385.

[9] ARPA, unpublished data.

[10] O.L. Murphy, G.D. Hitchens and D.J. Manko, *J. Power Sources, 47* (1994) 353–368.

[11] K. Prater, *J. Power Sources, 29* (1990) 239–250.